J. Am. Chem. Soc. **1987**, *109*, 6004-6010

Carbanion Spectroscopy: $^{-}CH_2NC$

**Sean Moran,[†] H. Benton Ellis, Jr.,[†,‡] D. J. DeFrees,[⊥] A. D. McLean,[§]
Suzanne E. Paulson,[†,∥] and G. Barney Ellison*[†]**

Contribution from the Department of Chemistry and Biochemistry, University of Colorado, Boulder, Colorado 80309-0215. *Received February 19, 1987*

Abstract: Photoelectron spectroscopy has been used to measure the electron affinities of the isocyanomethyl radicals: EA(CH_2NC) = 1.059 ± 0.024 eV and EA(CD_2NC) = 1.070 ± 0.024 eV. A Franck–Condon analysis of our spectra suggests that the isocyanomethide anion ($^{-}CH_2NC$) is a pyramidal species and a localized ion. This ion is bent out of the plane by 56 ± 5° with an inversion barrier of 650 ± 50 cm^{-1}. These structural conclusions are examined by a series of ab initio Hartree–Fock and Møller–Plesset perturbation calculations on both the isocyanomethyl radical and isocyanomethide ion. Using the gas-phase acidity of CH_3NC, we obtain the following bond-dissociation energy: $DH°_{298}(H{-}CH_2NC)$ = 84.8 ± 3.1 kcal/mol. These results are used to compute the isomerization energies for $^{-}CH_2NC \rightarrow CH_2CN^{-}$ and $CH_2NC \rightarrow CH_2CN$. These values are compared to other isocyano/cyano isomerizations.

I. Introduction

In the preceding paper,[1] we examined the photoelectron spectroscopy of the cyanomethide ion and used these results to discuss the structure and bonding of CH_2CN and CH_2CN^{-}. We now turn our attention to an isomeric ion, the isocyanomethide anion ($^{-}CH_2NC$). This ion might be written as $^{-}CH_2{-}N^{+}{\equiv}C{:}^{-}$ and thus one might conjecture that isocyanomethide will be a nonplanar species. How it relates to CH_3^{-} which is pyramidal[2] or to the essentially planar ion, $CH_2{=}C{=}N^{-}$, will be quite interesting. Dynamicists have long been intrigued by the isomerization[3-7] of $CH_3{-}NC$ to $CH_3{-}CN$ and the transformation of the allylic isocyanide,[8] $CH_2{=}CH{-}CH_2{-}NC$, to $CH_2{=}CH{-}CH_2{-}CN$. Interest in these overtone-induced isomerizations shows no sign of abating.[9,10] How is this rearrangement modified when one goes from the closed-shell neutral CH_3NC to the closed-shell ion, $^{-}CH_2NC$, or if one considers the open-shell radical, CH_2NC? In order to frame these questions better, we would like to consider the isomerizations of the negative ion

$$^{-}CH_2NC \rightarrow CH_2CN^{-} \qquad (1)$$

and the radical

$$CH_2NC \rightarrow CH_2CN \qquad (2)$$

We have studied the photoelectron spectra of the isocyanomethide ions, $^{-}CH_2NC$ and $^{-}CD_2NC$. We report the electron affinity of isocyanomethyl radical and a determination of the molecular geometry of CH_2NC and $^{-}CH_2NC$. From our spectroscopic determinations and the gas-phase acidity measurements[11] of CH_3NC, we have determined the enthalpy change for reactions 1 and 2. We have also completed ab initio molecular orbital calculations on the radical and the anion in order to aid in the interpretation of the photoelectron results and to establish the energies of (1) and (2) along with their activation energies.

II. Experimental Section

We have used the technique of photoelectron spectroscopy to study the isocyanomethide ion. The experimental technique has been reviewed[12,13] and a complete description of our spectrometer has been published.[14,15] The essence of the experiment is to prepare ion beams of an ion M^{-} and to irradiate them with a fixed-frequency, CW laser. One measures the kinetic energy (KE) of the scattered electrons.

$$M^{-} + \hbar\omega_0 \rightarrow M + e^{-}(KE) \qquad (3)$$

We prepare the ions in a high-pressure (roughly 0.2 Torr), magnetically confined plasma. For these spectra we use water and methyl isocyanide[16] to produce ions of m/z 40; employment of a 0.015-in. Ta filament and a 10-mA emission current produces intense (approximately 1 nA) negative ion beams. All of the negative ions are extracted from our source, velocity selected by a Wien filter, and delivered to an ultrahigh-vacuum (10^{-9} Torr) chamber for detachment. The details of the means by which we collect and calibrate our spectra are set forth in the preceding CH_2CN^{-} paper.[1]

III. Results

Our goal is to produce ion beams of $^{-}CH_2NC$ and to scrutinize the spectrum of this negative ion. Figure 1 depicts the photoelectron spectrum of the m/z 40 ion that results from using CH_3NC as a source gas in our spectrometer. This spectrum looks like it contains more than one Franck–Condon profile. Comparison of Figure 1 with the spectrum of CH_2CN^{-} (Figure 1 of

---

[†] Department of Chemistry, University of Colorado, Boulder, CO 80309-0215.

[‡] Present address: Department of Astronomy, University of Texas, Austin, TX 78712.

[⊥] Molecular Research Institute, Palo Alto, CA 94304.

[§] IBM Almaden Research Center, San Jose, CA 95120-6099.

[∥] Present address: Department of Environmental Engineering, California Institute of Technology, Pasadena, CA 91125.

(1) Moran, S.; Ellis, H. B., Jr.; DeFrees, D. J.; McLean, A. D.; Ellison, G. B. *J. Am. Chem. Soc.* preceding paper in this issue.

(2) Ellison, G. B.; Engelking, P. C.; Lineberger, W. C. *J. Am. Chem. Soc.* **1978**, *100*, 2556.

(3) Harris, H. H.; Bunker, D. L. *Chem. Phys. Lett.* **1971**, *11*, 433.

(4) Bunker, D. L.; Hase, W. L. *J. Chem. Phys.* **1973**, *59*, 4621.

(5) Redmon, L. T.; Purvis, G. D.; Bartlett, R. J. *J. Chem. Phys.* **1978**, *69*, 5386.

(6) Saxe, P.; Yamaguchi, Y.; Pulay, P.; Schaefer, H. F., III *J. Am. Chem. Soc.* **1980**, *102*, 3718.

(7) Reddy, K. V.; Berry, M. J. *Chem. Phys. Lett.* **1977**, *52*, 111.

(8) Reddy, K. V.; Berry, M. J. *Chem. Phys. Lett.* **1979**, *66*, 223.

(9) Snavely, D. L.; Zare, R. N.; Miller, J. A.; Chandler, D. W. *J. Chem. Phys.*, submitted for publication.

(10) Miller, J. A.; Chandler, D. W. *J. Chem. Phys.*, submitted for publication.

(11) Filley, J.; DePuy, C. H.; Bierbaum, V. M. *J. Am. Chem. Soc.*, preceding in this issue.

(12) Drazaic, P. S.; Marks, J.; Brauman, J. I. In *Gas Phase Ion Chemistry*; Bowers, M. T., Ed.; Academic: New York, 1984; Vol. 3, Chapter 21.

(13) Mead, R. D.; Stevens, A. E.; Lineberger, W. C. In *Gas Phase Ion Chemistry*; Bowers, M. T., Ed.; Academic: New York, 1984; Vol. 3, Chapter 22.

(14) Ellis, H. B., Jr. Ph.D. Thesis, University of Colorado, 1983.

(15) Ellis, H. B., Jr.; Ellison, G. B. *J. Chem. Phys.* **1983**, *78*, 6441.

(16) Our sample of CH_3NC was prepared and characterized by standard methods: Schuster, R. E.; Scott, J. E.; Casanova, J., Jr. In *Organic Syntheses*; Baumgarten, H. E., Ed.; John Wiley: New York, 1973; pp 772–774.

(17) Costain, C. C. *J. Chem. Phys.* **1958**, *29*, 864.

(18) MacKenzie, M. W.; Duncan, J. L. *J. Mol. Struct.: THEOCHEM* **1982**, *95*, 245.

(19) Vincent, M. A.; Dykstra, C. E. *J. Chem. Phys.* **1980**, *73*, 3838.

(20) Ichikawa, K.; Hamada, Y.; Sugawara, Y.; Tsuboi, M.; Kato, S.; Morokuma, K. *Chem. Phys.* **1982**, *72*, 301.

(21) Hopkinson, A. C.; McKinney, M. A.; Lien, M. H. *J. Comput. Chem.* **1983**, *4*, 513.

(22) Lien, M. H.; Hopkinson, A. C.; McKinney, M. A. *J. Mol. Struct.: THEOCHEM* **1983**, *105*, 37.

(23) Kaneti, J.; Schleyer, P. v. R.; Clark, T.; Kos, A. J.; Spitznagel, G. W.; Andrade, J. G.; Moffat, J. B. *J. Am. Chem. Soc.* **1986**, *108*, 1481.

(24) Swanton, D. J.; Bacskay, G. B.; Willett, G. D.; Hush, N. S. *J. Mol. Struct.: THEOCHEM* **1983**, *91*, 313.

(25) This work.

(26) Hinchliffe, A. *J. Mol. Struct.* **1979**, *53*, 147.

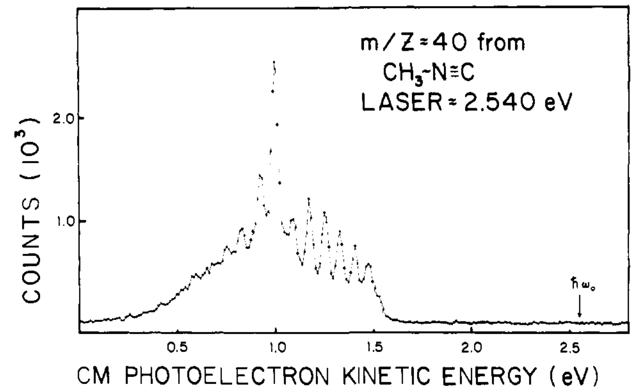

Figure 1. A fast scan of the photoelectron spectrum of the *m/z* 40 ions produced by electrical discharge of CH_3NC. The data points are separated by roughly 10 meV; the energy of the laser is 2.540 eV and is marked by $\hbar\omega_0$.

ref 1) immediately suggests that the intense, sharp feature at around 1.0 eV belongs to the cyanomethide ion. The CH_2CN^- ion is also most likely the carrier of the signal in Figure 1 for all features between 0 and 1 eV. The spectrum of CH_2CN^- is transparent[1] at CM kinetic energies above 1.05 eV. Figure 1 could be interpreted in two different ways. (a) Use of CH_3NC as an ion precursor generates ion beams of CH_2CN^- that are highly vibrationally excited. Detachment of these chemically activated ions produces a photoelectron spectrum with a set of intense hot bands. (b) The spectrum in Figure 1 results from the blending together of two isomeric ions both of which have *m/z* 40. The plasma discharge source might isomerize the CH_3NC to acetonitrile; proton abstraction from CH_3CN would then produce the cyanomethide ion. Consequently Figure 1 displays the photoelectron spectra of CH_2CN^- and $^-CH_2NC$ blended together. The features belonging to the cyanomethide ion can be identified from their known transition energies[1] and the remaining signals would then be attributed to the isocyanomethide ion, $^-CH_2NC$.

We are certain that interpretation (b) is the correct one. From the experimental constants[1] for CH_2CN^- it is extremely unlikely that the spectral features in Figure 1 between 1.0 and 1.5 eV could result from detachment of vibrationally excited CH_2CN^- ions. In a parallel set of experiments, the isocyanomethide ion has been prepared in a flowing afterglow device.[11] These gas-phase, afterglow studies show that NH_2^- and several other bases will abstract a proton from CH_3NC to produce $^-CH_2NC$. The chemistry of the isocyanomethide ion is quite different from that of CH_2CN^-; for example, $^-CH_2NC$ reacts with O_2 while CH_2CN^- does not. The isomeric ions $^-CH_2NC$ and CH_2CN^- are distinct, non-interconverting species in the flow tube. Charge-transfer studies in the flowing afterglow device were used[11] to qualitatively bracket the EA(CH_2NC); it is found that EA(CH_2NC) = 0.8 ± 0.4 eV. This is entirely consistent with our spectrum in Figure 1. The features between 1.0 and 1.5 eV are all assigned as belonging to the $^-CH_2NC$ ion.

Slow scans of the origin are shown in Figures 2 ($^-CH_2NC$) and 3 ($^-CD_2NC$). Each of the features of these spectra (z, Z, Y, ..., A) are collected in Table I. The peak A is the (0,0) transition of the CH_2CN^- spectrum; this is the feature also labeled A in ref 1.

Comparison of Figures 2 and 3 suggests that peak Z is the origin of the isocyanomethide spectrum. In $^-CD_2NC$, all of the features Y, X, W, ... collapse to higher CM kinetic energies while the blended z peak moves to lower kinetic energies. All features seem to shift toward the Z peak and this is a distinguishing mark of the (0,0) transition. When the fact that the laser energy is 2.540 eV is used, this implies that the uncorrected or raw electron affinities are raw EA(CH_2NC) = 1.067 ± 0.024 eV and raw EA(CD_2NC) = 1.078 ± 0.024 eV.

IV. Discussion

A. Identity of the Active Modes. Before proceeding to assign the transitions in Figures 2 and 3, it is useful to survey the facts about the geometry of $^-CH_2NC$ and CH_2NC. Table II collects together the experimentally determined geometry of CH_3NC and the results of several ab initio calculations on H_2N–NC, $^-CH_2NC$, and CH_2NC. As near as we are aware there is no experimental information available for the isocyanomethide ion or the isocyanomethyl radical. Isocyanamide H_2N–NC, is the neutral molecule isoelectronic to the ion, $^-CH_2NC$; consequently it is included in Table II and likewise there are no experimental data.

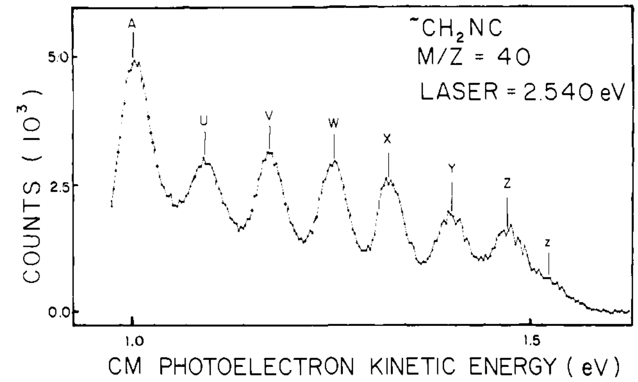

Figure 2. A slow scan of the photoelectron spectrum of $^-CH_2NC$. The data points are separated by roughly 2.8 MeV. Values of the peak positions (z–A) are collected in Table I.

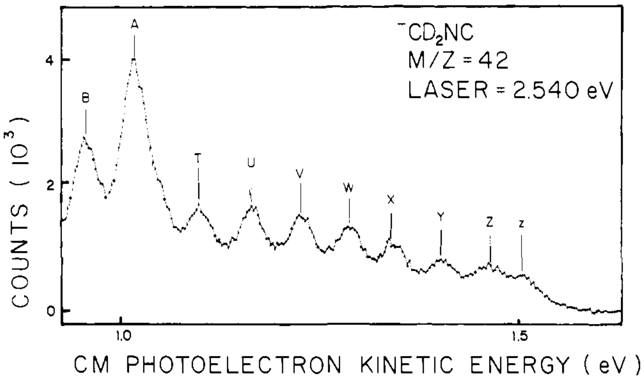

Figure 3. A slow scan of the photoelectron spectrum of $^-CD_2NC$. The data points are separated by roughly 2.8 meV. Values of the peak positions (z–B) are colleced in Table I.

Table I. Measured CM Kinetic Energy (eV) for Isocyanomethide Ions (Laser λ_0 = 488.0 nm (2.540 eV))

Peak	$^-CH_2NC$	$^-CD_2NC$
z	1.523 ± 0.024	1.503 ± 0.020
Z	1.473 ± 0.024	1.462 ± 0.024
Y	1.399 ± 0.017	1.402 ± 0.018
X	1.322 ± 0.016	1.341 ± 0.016
W	1.253 ± 0.014	1.285 ± 0.013
V	1.173 ± 0.014	1.221 ± 0.014
U	1.092 ± 0.012	1.156 ± 0.013
T		1.099 ± 0.014
A	1.004 ± 0.012	1.018 ± 0.013
B	0.928 ± 0.018	0.957 ± 0.014

Table II suggests that there will be significant geometry changes between the isocyanomethide ion and the isocyanomethyl radical. The calculations of ref 23 or 25 (for example) find Δr(H_2C–N) = 0.08 Å, $\Delta\alpha$(HCH) = 14°, and $\Delta\alpha$(HCN) = 11°, and $\Delta\xi$ = 59°. This implies that there may be several active modes excited upon detachment. The analogous geometric changes computed between CH_2CN and CH_2CN^- are significantly less.[1]

In our study of the cyanomethide ion we found that we could model detachment of the CH_2CN^- ion with the umbrella-like vibration (ω_5) as the sole active mode. In order to have a uniform set of predictions about the properties of CH_2NC and $^-CH_2NC$, we have carried out a set of ab initio calculations on both species.

B. Computational Results. Our ab initio molecular orbital calculations on the isocyanomethyl radical and the isocyano-

Table II. Experimental and ab Initio Geometrical Constants[a]

species	r(NC)	r(H_2C-N)	r(CH)	α(HCH)	α(HCN)	α(CNC)	ζ	b	ref
CH_3NC	1.166	1.424	1.101	109.8	109.1	180			17, 18
NH_2NC	1.169	1.352	0.997	111.4	108.3	176.9	55.3	2090	19
NH_2NC	1.151	1.355	1.001	109.1	108.3	175.6	57.3	2245	20
NH_2NC	1.151	1.354	1.001	109.3	108.5	175.6	56.8	2083	25
$^-CH_2NC$	1.165	1.506	1.109		100.9	180			21
$^-CH_2NC$	1.166	1.452	1.088	109	108.4	176.3	55	1924	22
$^-CH_2NC$	1.154	1.431	1.090	109.9	107.4	175.8	58.6	980	23
$^-CH_2NC$	1.176	1.372	1.070	122.2	118.9	180			24
$^-CH_2NC$	1.154	1.431	1.089	109.1	107.4	175.8	59.0	1642	25
CH_2NC	1.22	1.35	1.11	119	121	180	0	0	26
CH_2NC	1.165	1.366	1.071	119.9	120.1	180			24
CH_2NC	1.167	1.349	1.070	122.9	118.5	180	0	0	25

[a] Distances in Å. α and ζ in deg. b in cm^{-1}.

Table III. ab Initio Calculated Properties

I. Energies

CH_2NC (C_{2v})

A. Total Energy:
[UHF/6-31+G(d)] = −131.27693 hartrees
[MP2/6-311++G(d,p)] = −131.70252 hartrees
["MP4/6-311++G(d,p)"] = −131.74452 hartrees
B. Harmonic Vibrational Frequencies (cm^{-1}) from a Scaled [UHF/-31+G(d)] Calculation:
$\omega_7 = 3106$, $\omega_1 = 2987$, $\omega_2 = 1961$, $\omega_3 = 1420$, $\omega_8 = 1093$, $\omega_4 = 1009$, $\omega_5 = 373$, $\omega_6 = 351$, $\omega_9 = 274$
C. Rotational Constants [UHF/6-31+G(d)]
$A = 9.460\ cm^{-1}$, $V = 0.381\ cm^{-1}$, $C = 0.367\ cm^{-1}$

$^-CH_2NC$ (C_s)

A. Total Energy:
[RHF/6-31+G(d)] = −131.25891 hartrees
[MP2/6-311++G(d,p)] = −131.78011 hartrees
["MP4-3-311++G(d,p)"] = −131.74160 hartrees
B. Harmonic Vibrational Frequencies (cm^{-1}) from a Scaled [RHF/6-31+G(d)] Calculation:
$\omega_7 = 2827$, $\omega_1 = 2787$, $\omega_2 = 2100$, $\omega_3 = 1430$, $\omega_8 = 1182$, $\omega_4 = 922$, $\omega_5 = 682$, $\omega_6 = 415$, and $\omega_9 = 326$
C. Rotational Constants [RHF/6-31+G(d)]
$A = 8.207\ cm^{-1}$, $B = 0.365\ cm^{-1}$, $C = 0.356\ cm^{-1}$

II. Geometrical Constants [UHF/6-31+G(d)][a]

species	r(NC)	r(C–NC)	r(CH)
CH_2NC	1.167	1.349	1.070
$^-CH_2NC$	1.154	1.431	1.089

species	α(HCH)	α(HCN)	α(CNC)	ζ	b
CH_2NC	122.9	118.5	180	0	0
$^-CH_2NC$	109.1	107.4	175.8	59.0	1642

[a] Bond lengths in Å; b is the inversion barrier in cm^{-1}. α and ζ are in deg. The correlated MP2/6-31+G(d) values for ζ and b of the anion are in much better accord with experiment than the Hartree–Fock values, see sections IV.B and IV.C.

methide anion, Table III, were performed by using the methods detailed in the accompanying paper[1] on CH_2CN^-. Geometries were optimized and harmonic vibrational frequencies were computed at the Hartree–Fock (HF), self-consistent-field (SCF) level with the 6-31+G(d) basis set;[27] the vibrational frequencies were then scaled[28] by 0.89. The spin-unrestricted, UHF, wave function used for the radical is not an eigenfunction of the spin-squared operator, S^2, and it can be contaminated by quartets, sextets, etc., possibly leading to errors in the computed properties that are larger than in uncontaminated cases.[29] For CH_2NC $\langle S^2 \rangle$ is 0.82 compared to 0.92 for[1] CH_2CN and 0.75 for a pure doublet. Thus, while the errors due to spin contamination would be anticipated, they might be expected to be smaller than those for the cyanide.

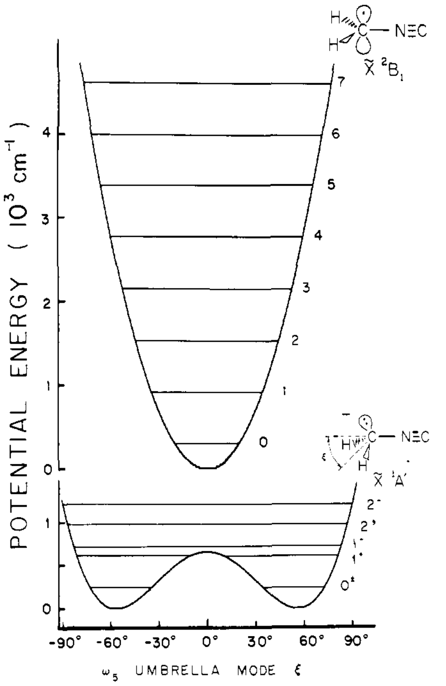

Figure 4. Curves used to model the asymmetric umbrella potential (ω_5) of $^-CH_2NC$ and CH_2NC. The vibrational energy levels are calculated by variationally solving a model hamiltonian (Table III). The inversion barrier is only 650 cm^{-1} in the carbanion so each of the vibrational levels is split into a pair of levels; these are labeled $0^{\pm}$, 1^+, 1^-, etc. The CH_2NC radical is a planar species with little or no inversion barrier.

The inversion barrier, b, for the anion (Table III) and for the isoelectronic species isocyanide (Table II) was computed by optimizing the geometry in a planar, C_{2v} configuration; vibrational frequencies computed for these structures show a single, out-of-plane imaginary frequency, correct for a transition state. The inversion barrier was also computed at the correlated MP2/6-31+G(d)[30] level, which gave a more accurate value than did HF/6-31+G(d) for CH_2CN^-. For $^-CH_2NC$ the resultant inversion barrier is 1029 cm^{-1} and the out-of-plane bending angle ξ (Figure 4) is 52.2°.

The approximate local-mode descriptions of the normal modes given in Table III of the CH_2CN^- paper[1] for CH_2CN apply to the analogous CH_2NC ab initio modes. However, several of the normal modes in $^-CH_2NC$ differ from the descriptions given in that table because the molecule is pyramidal rather than planar. In particular, the C–N single-bond stretching motion and the umbrella motion are mixed in the anion whereas for CH_2NC they are distinct. In the radical ω_4 is the C–N stretch and ω_5 is the umbrella motion; but in the anion ω_4 is primarily the C–N stretch with some umbrella motion mixed in and ω_5 is primarily the umbrella motion with some C–N stretch mixed in.

---

(27) (a) Hariharan, P. C.; Pople, J. A. *Theor. Chim. Acta* **1973**, *28*, 213. (b) Clark, T.; Chandrasekhar, J.; Spitznagel, G. W.; Schleyer, P. v. R. *J. Comput. Chem.* **1983**, *4*, 294.

(28) (a) Pople, J. A.; Schlegel, H. B.; Krishnan, R.; DeFrees, D. J.; Binkley, J. S.; Frisch, M. J.; Whiteside, R. A.; Hout, R. F., Jr.; Herhe, W. J. *Int. J. Quantum Chem., Quantum Chem. Symp.* **1981**, *15*, 269. (b) DeFrees, D. J.; McLean, A. D. *J. Chem. Phys.* **1985**, *82*, 333.

(29) Farnell, L.; Pople, J. A.; Radom, L. *J. Phys. Chem.* **1983**, *87*, 79.

(30) (a) Møller, C.; Plesset, M. S. *Phys. Rev.* **1934**, *46*, 618. (b) Pople, J. A.; Binkley, J. S.; Seeger, R. *Int. J. Quantum Chem., Symp.* **1976**, *10*, 1.

Single-point calculations at higher levels of theory were used to estimate the proton affinity of $^-CH_2NC$. The relevant MP2/6-311++D(d,p) total energies, shown in Table III, were computed at the UHF/6-31+G(d) geometries. This type of calculation provides particularly accurate predictions of absolute proton affinities (PA): $^-CH_2NC + H^+ \rightarrow CH_3NC$. When applied to several small neutral and anionic molecules the error was roughly ±4 kcal/mol.[31] For example, the PA for cyanide, CN^-, is predicted to be 351.3 kcal/mol compared to the experimental value[31,32] of 349.4 ± 1.8. The absolute proton affinity computed for $^-CH_2NC$ with scaled 6-31+G(d) vibrational frequencies for the vibrational energies[33] is 383 kcal/mol. This agrees with the value of 380 kcal/mol computed earlier[23] with second-order perturbation theory with a smaller basis set (MP2/6-31+G(d)), an empirical value for the zero-point correction, and the observed PA of CH_3^-. These theoretical values do not agree, except perhaps at the extreme limits of the estimated errors, with the measured value of 374 ± 3 kcal/mol.[11] Clearly, calculations with more accurate theoretical methods as well as independent experimental determinations of this value are needed to resolve the discrepancy.

Single-point calculations with larger basis sets and higher order correlation corrections were also performed to estimate the energies of isomerization and the energies of activation for a series of cyano/isocyano transformations. These were done at the "MP4/6-311++G(d,p)" level with 6-31+G(d) geometries and scaled vibrational frequencies. The quotations show that this level of calculations was approximated by using a technique that has been shown to lead to small errors.[34] The results of these calculations are shown in Table VI; the geometries, frequencies, and total energies used in deriving these results will be published separately.[35]

C. Quantitative Modeling of the Franck–Condon Profile. We now turn our attention to the precise assignment of the spectroscopic features in Figures 2 and 3. From the data in Table I, it seems apparent that one single mode is excited upon detachment of the $^-CH_2NC$ ion. This is a low-frequency vibration being about 600 cm^{-1} in the isocyanomethyl radical and 400 cm^{-1} in the isocyanomethide anion. The spectrum of the $^-CD_2NC$ ion indicates that this vibration strongly involves the C–H bonds since both of the frequencies drop by roughly 20%.

A pronounced difference between the calculated geometries of the ion and the radical in Table III is the out-of-plane bending angle, ξ. The CH_2NC radical is predicted to be a planar, C_{2v} species while the $^-CH_2NC$ ion is predicted to be a pyramidal molecule. The ion is calculated at the HF/6-31+G(d) level to be bent at an angle $\xi = 59°$ with a barrier to inversion of 1642 cm^{-1}. On account of our ab initio calculations and because we were so successful in modeling our CH_2CN^- spectra with the umbrella mode alone,[1] we will strive to interpret the spectra in Figures 2 and 3 as arising from excitation of the low-frequency ω_5 mode. As discussed above, the qualitative vibrational modes for CH_2NC are quite similar to those for CH_2CN listed in Table III of ref 1 and the ω_5 oscillator is the umbrella mode in the isocyanomethyl radical and the isocyanomethide ion.

A convenient potential to represent an umbrella vibration is a linear oscillation perturbed by a Gaussian barrier.[36] Table IV collects together a set of parameters of the active mode in CH_2NC and $^-CH_2NC$. Figure 4 is a plot of the potentials $[V(Q_5)]$ that we have employed for both species. To construct these potentials, we used the ab initio results from Table III to make conjectures about the parameters K_5, C, β, b, and ξ for the CH_2NC radical. These were varied until we could reproduce the radical splittings (Z,Y), (Y,X), (X,W), (W,V), and (V,U). For the $^-CH_2NC$ ion we have consulted Table III again and made use of the hot band frequency (z,Z).

Table IV. Vivrational Schrödinger Equation (H_2C–NC Umbrella Mode (ω_5))

A. Formulae

$$V(Q_5) = 0.5k_5Q_5^2 + C\exp(-\beta Q_5^2)$$
$$g_{55} = (M_C + M_N)^{-1} + (M_C)^{-1} + (M_C/2)(X/Z) + [(2M_H + M_C)/(2M_HM_C)](X/Z)^2$$

where:

$Q_5(\zeta) = [\pi_{180}]X\zeta$; $X = r_{C\text{-}NC}$

α_0 = H–C–H angle; $Z = r_{CH}\cos(\alpha_0/2)$

$\rho = \ln[2C\beta/k_5]$

$\zeta_{min} = (180/\pi X)[\rho/\beta]^{3/2}$; barrier $= b = C(e^{\rho} - \rho - 1)e^{-\rho}$

B. Fitting Parameters[a]

radical	anion
$r_{C\text{-}H}' = 1.10$ Å	$r_{C\text{-}H}'' = 1.10$ Å
$r_{C\text{-}NC}' = 1.42$ Å	$r_{C\text{-}NC}'' = 1.42$ Å
$\alpha_0' = 120°$	$\alpha_0'' = 109°$
$k_5' = 2541$ cm^{-1} Å^{-2}	$k_5'' = 3735$ cm^{-1} Å^{-2}
$C' = 0$ cm^{-1}	$C'' = 15669$ cm^{-1}
$\beta' = 0$ Å^{-2}	$\beta'' = 0.164$ Å^{-2}
$\zeta_{mi(}' = 0 \pm 5°$	$\zeta_{min}'' = 56 \pm 5°$
$b' = 0 \pm 50$ cm^{-1}	$b'' = 650 \pm 50$ cm^{-1}.

[a] During the fit of $V(Q_5)$, $r_{C\text{-}H}$, $r_{C\text{-}NC}$, and α_0 are constrained.

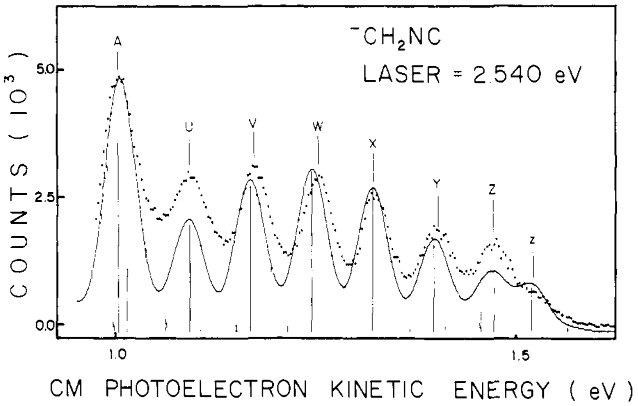

Figure 5. A high signal-to-noise photoelectron spectrum of $^-CH_2NC$. The points are the experimental spectrum from Figure 2 while the solid line is a calculated spectrum for comparison. The modeled spectrum results from a Franck–Condon calculation with use of the potential curves in Figure 3.

The calculation of the vibrational frequencies and wave functions for the ion and radical means that we must set up and solve a vibrational Schrödinger equation for each species. We will assume that each of the vibrational modes is independent and can be solved for separately. We will approximate the active mode as a local mode (Ω_{vib}) and attempt to calculate them from the following vibrational Schrödinger equation.[37]

$$[{}^1\!/\!_2 g_{55}\hbar^2\, \partial^2/\partial Q_5^2 + V(Q_5)]\Omega_{vib}(Q_5) = E_v\Omega_{vib}(Q_5) \qquad (4)$$

Equation 4 describes the v-th vibrational state, $\Omega_{vib}(Q_5)$. The effective mass of the oscillator is given by the reciprocal of the Wilson **g**-matrix element, g_{55}, and $V(Q_5)$ is the vibrational potential function. The potentials $V(Q_5)$ for the isocyanomethyl radical and the isocyanomethide ion are shown in Table IV.

By variationally solving the Schrödinger equations (4), we can construct the Franck–Condon profile for detachment of $^-CH_2NC$. The results of our modeling calculations are shown in Figure 5 where the points are the experimental data (from Figure 2) and the solid line is the calculated Franck–Condon factors (sticks)

---

(31) DeFrees, D. J.; McLean, A. D. *J. Comput. Chem.* **1986**, *7*, 321.

(32) (a) Bartmess, J. E.; Scott, J. A.; McIver, R. T., Jr. *J. Am. Chem. Soc.* **1979**, *101*, 6046. (b) Betowski, D.; Mackay, G.; Payzant, J.; Bohme, D. *Can. J. Chem.* **1975**, *53*, 2365. (c) Chase, M. W., Jr.; Curnutt, J. L.; Downey, J. R. *Jr.*: McDonald, R. A.; Syverud, A. N.; Valenzuela, E. A. *J. Phys. Chem. Ref. Data* **1982**, *11*, 695.

(33) For methyl isocyanide the MP2/6-311++G(d,p)//6-31+G(d) energy is −132.36548 hartrees and the scaled 6-31+g(d) zero-point vibrational energy is 27.2 kcal/mol.

(34) Frisch, M. J.; Binkley, J. S.; Schaefer, H. F., III *J. Chem. Phys.* **1984**, *81*, 1882.

(35) Whiteside, R. A.; Frisch, M. J.; DeFrees, D. J.; Raghavachari, K.; Binkley, J. S.; Schlegel, H. B.; Pople, J. A. *The Carnegie-Mellon Quantum Chemistry Archive*, Pittsburgh, PA.

(36) Coon, J. B.; Naugle, N. W.; McKenzie, R. D. *J. Mol. Spectrosc.* **1966**, *20*, 107.

(37) Wilson, E. B.; Decius, E. C.; Cross, P. C. *Molecular Vibrations*; McGraw-Hill: New York, 1955; Appendix VI.

Table V. Experimental Molecular Properties

	radical[a]		anion[b]	
	CH_2NC	CD_2NC	$^-CH_2NC$	$^-CD_2NC$
ω_5[c]	615	486	374	335
$0^{\pm}$ inversion splitting[c]	0	0	5	1
inversion barrier	0 ± 50		650 ± 50	
ζ_{min}[b]	0 ± 5		56 ± 5	
A[c]	9.22 ± 0.48	4.61 ± 0.24	8.07 ± 0.28	4.18 ± 0.17
B[c]	0.359 ± 0.040	0.318 ± 0.040	0.366 ± 0.010	0.327 ± 0.001
C[c]	0.346 ± 0.040	0.297 ± 0.040	0.357 ± 0.001	0.312 ± 0.001
asymmetry constant	−0.997	−0.990	−0.998	−0.992
$\Delta H°_{f298}$[e]	74.0 ± 3.1		49.6 ± 3.1	

[a] $EA(CH_2NC) = 1.059 \pm 0.024$ eV. $\Delta H°_{acid}(H{-}CH_2NC) = 374 \pm 3$ kcal/mol. [b] $EA(CD_2NC) = 1.070 \pm 0.024$ eV. $DH°_{298}(H{-}CH_2NC) = 84.8 \pm 3.1$ kcal/mol. [c] cm^{-1}. [d] deg. [e] kcal/mol.

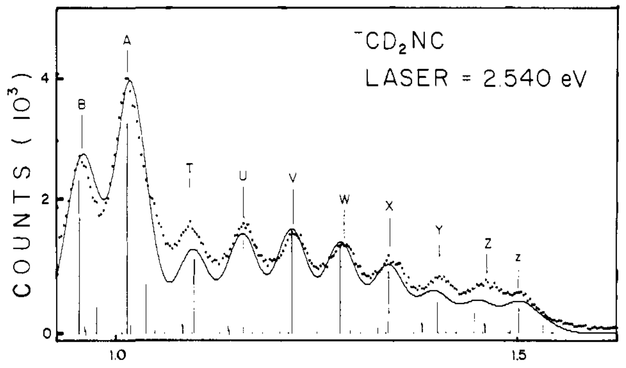

Figure 6. A high signal-to-noise photoelectron spectrum of $^-CD_2NC$. The points are the experimental spectrum from Figure 3 while the solid line is a calculated spectrum for comparison. The modeled spectrum results from a Franck–Condon calculation with use of the potential curves in Figure 3.

folded with an experimental line width. To test our potentials for ω_5 for the radical and the ion (Table IV), we should consider the $^-CD_2NC$ ion. Within the Born–Oppenheimer approximation, we should be able to predict the detachment spectrum of the deuteriated ion with the potentials in Table IV by simply substituting the **g**-matrix element with M_D for M_H. A comparison of our calculated Franck–Condon profile with the experimental data is provided in Figure 6.

We conclude that the simple potentials in Table IV provide a solid basis to describe the vibrational activity induced in CH_2NC by detachment of the $^-CH_2NC$ ion. The fundamental vibrational frequency is found to be $\omega_5(CH_2NC) = 615$ cm^{-1} while $\omega_5(^-CH_2NC) = 374$ cm^{-1}. It is evident that the agreement with the harmonic ab initio values of Table III [$\omega_5^{har}(CH_2NC) \simeq 373$ cm^{-1} and $\omega_5^{har}(^-CH_2NC) \simeq 682$ cm^{-1}] is disappointing. Further calculations are needed to determine to what extent the discrepancy is due to deficiencies in the computational model. For CH_2NC the effect of spin contamination needs to be explored. For $^-CH_2NC$ the effect of correlation on the barrier height suggests that this be determined for the frequencies as well.

From Figures 5 and 6, we find that the isocyanomethyl radical is a planar species while the ion is a pyramidal molecule. The $^-CH_2NC$ ion is bent out of the plane by $\xi = 56 \pm 5°$ and has an inversion barrier of $b = 650 \pm 50$ cm^{-1}. The ab initio values at the MP2/6-31+G(d) level are in reasonable accord with these results; as with CH_2CN^- the SCF barrier height does not agree with the observed value. Rotational constants derived from the parameters in Table IV all indicate that both the radical and the ion are nearly prolate symmetric tops. Many of these experimentally derived parameters are tabulated in Table V.

D. GVB Models. We would like to develop a simple picture of the CH_2NC and $^-CH_2NC$. First consider the simpler molecule hydrogen isocyanide, HNC, in Figure 7. We will use a GVB picture to develop these ideas.[38,39] Suppose we construct CNH by combining C (^3P) with NH ($X^3\Sigma^-$). This leads to a bent triatomic molecule, CNH ($^1A'$), with a double bond, C=N. Alternatively we might use NH ($A^3\Pi$); the A state of NH is 29 807.4 cm^{-1} above the ground X state.[40] This leads to a linear molecule, CNH ($^1\Sigma^+$). Because the CNH correlated ($2s^2 \rightarrow 2p^2$) lobe pair (bottom left, Figure 7) can pooch out of the way of the N π^2 electron pair, linear CNH can delocalize to form a partial triple carbon to nitrogen bond. The real structure of CNH is likely to be somewhere between these two formulae. This picture suggests that CNH will have a longer NC bond length and a lower NC stretching frequency than HCN. Since CNH ($\tilde{X}^1\Sigma^+$) continuously deforms into the bent CNH structure (Figure 7, top), the bending vibration of CNH is likely to be dramatically lower than that of HCN.

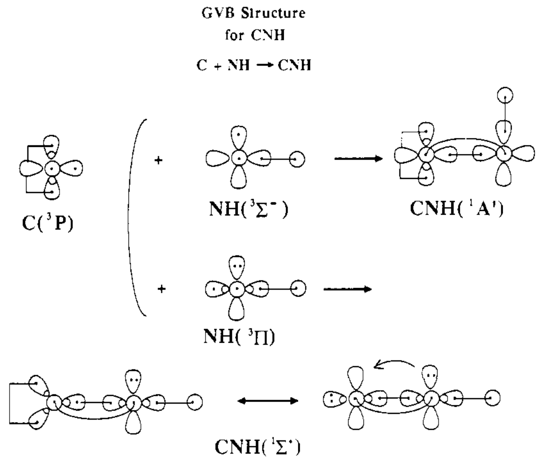

Figure 7. GVB diagrams showing the formation of CN–H from the ground state of C (^3P) and the lowest two excited states of NH. Bonding of the C atom to the out-of-plane π orbital of NH $X(^3\Sigma^-)$ would lead to a doubly bonded, bent CNH species, $\tilde{X}(^1A_1)$. Alternatively, the C atom could combined with the σ orbital of an excited state of NH $A(^3\Pi)$ to produce a triply bonded, linear CNH molecule, $\tilde{X}(^1\Sigma^+)$.

Microwave spectroscopy has determined the relative structures of the HCN and HNC molecules[41-43] as HCN ($r_{HC} = 1.063$ Å; $r_{CN} = 1.155$ Å) and HNC ($r_{HN} = 0.987$ Å; $r_{NC} = 1.171$ Å). The vibrational modes of HCN and CNH have been summarized[44,45] as HCN [$\omega_1 = 3442.3$ cm^{-1}, $\omega_2 = 2129.1$ cm^{-1}, and $\omega_3 = 727.0$ cm^{-1}] and CNH [$\omega_1 = 3620$ cm^{-1}, $\omega_2 = 2020.5$ cm^{-1}, and $\omega_3 = 477$ cm^{-1}]. The HNC dative π bond can explain the longer HN=C bond and lower ω_2 frequency. The bending frequency

---

(38) Goddard, W. A., III; Dunning, T. H., Jr.; Hunt, W. J.; Hay, P. J. *Acc. Chem. Res.* **1973**, *6*, 368.

(39) Goddard, W. A., III; Harding, L. B. *Annu. Rev. Phys. Chem.* **1978**, *29*, 363.

(40) Huber, K. P.; Herzberg, G. *Molecular Spectra and Molecular Structure IV. Constants of Diatomic Molecules*; Van Nostrand: New York, 1979.

(41) Creswell, R. A.; Pearson, E. F.; Winnewisser, M.; Winnewisser, G. *Z. Naturforsch. A: Phys., Phys. Chem. Kosmophys.* **1976**, *31A*, 221.

(42) Pearson, E. F.; Creswell, R. A.; Winnewisser, M.; Winnewisser, G. *Z. Naturforsch. A: Phys., Phys. Chem. Kosmophys.* **1976**, *31A*, 1394.

(43) Ghosh, S. N.; Trambarulo, R.; Gordy, W. *J. Chem. Phys.* **1953**, *21*, 308.

(44) Strey, G.; Mills, I. M. *Mol. Phys.* **1973**, *26*, 129.

(45) Creswell, R. A.; Robiette, A. G. *Mol. Phys.* **1978**, *36*, 869.

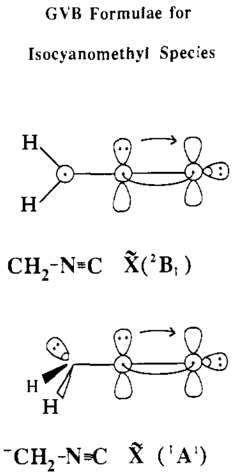

Figure 8. GVB diagrams describing the formation of the isocyanomethyl radical, CH_2NC, from ground-state CH_2 and NC ($B^2\Sigma^+$). Bonding of the NC radical to the out-of-plane π-like orbital of $\tilde{X}\,^3B_1$ methylene would lead to a nonplanar radical, CH_2NC ($\tilde{X}\,^2A'$). Alternatively, NC could combine with the in-plane lobe orbital of CH_2 to produce a planar radical, CH_2NC ($\tilde{X}\,^2B_1$). The only coupling likely between NC ($B^2\Sigma^+$) and CH_2^- to yield the carbanion is through the out-of-plane π-like orbital of $\tilde{X}\,^2B_1$ CH_2^-. This suggests the formation of a nonplanar ion, CH_2NC^- ($\tilde{X}\,^1A'$).

in CNH drops by 250 cm^{-1} with respect to ω_3(HCN).

Our picture of CNH in Figure 7 suggests that the molecular dipole moment, μ(CNH), should be less than μ(HCN). For HCN both the σ and π dipole components (μ_σ and μ_π) are directed toward the N end; experimentally[43] it is found that $|\mu(HCN)|$ = 2.975 ± 0.005 D. In figure 7 (bottom) is seems that μ_σ and μ_π will oppose each other CNH; the dipole moment of CNH has been estimated[46] to be $|\mu(CNH)|$ = 3.05 ± 0.1 D.

Similar arguments could be advanced for CH_3CN and CH_3NC. In this case we combine CH_3N with the C atom. The spectroscopy of CH_3N has recently been scrutinized[47] and the ground state is $\tilde{X}\,^3A_2$. The first excited triplet state is $\tilde{A}\,^3E$ at T_0 = 31 811 cm^{-1}. For acetonitrile and methyl isocyanate the dipole moments are known[43] more precisely: $|\mu(CH_3CN)|$ = 3.92 ± 0.06 D and $|\mu(CH_3NC)|$ = 3.83 ± 0.06 D. The model in Figure 7 is consistent with all of these results.

Let us now consider the isocyanomethyl radical and the isocyanomethide ion. In Figure 8 we can picture these species as being derived from the NC radical ($B^2\Sigma^+$) at T_0 = 25 752.0 cm^{-1} and either CH_2 or CH_2^-. The isocyanomethyl radical is pictured as a symmetric, planar species with the ground state as $\tilde{X}$ ($^2B_2$). In contrast the isocyanomethide anion should be a strongly pyramidal molecule, $\tilde{X}\,^1A'$. In both cases the "π-like" electron pair centered on the N atom is polarized back onto the terminal C atom. In contrast to the nearly planar CH_2CN^- ion, the isomeric ion is much more of a localized species which we write as $^{-}CH_2NC$.

There is earlier evidence to suggest that isocyanide anions might be considered to be localized ions. Isotope exchange studies[48] of 2,2-diphenylcyclopropyl isocyanide reveal that treatment of the isocyanide with t-BuO$^-$ in THF solution followed by quenching with t-BuOD (eq 5) leads to a product 98% optically pure with 98% deuterium incorporation. Treatment of the isomer, 2,2-diphenylcyclopropyl cyanide, produces a racemic mixture of deuteriated products. Equation 5 suggests that the isocyanide carbanion is configurationally stable in solution.

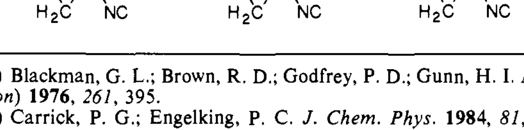

(5)

An interesting contrast between CH_2CN^- and $^{-}CH_2NC$ is the degree of charge delocalization. One can think of the isocyanomethide ion as a localized anion and we should consider the possibilities of this species as an α nucleophile. In a study of the chemistry of HOO^-, no unusual reactivity compared to HO^- could be found and it was concluded that the α-effect was most likely a manifestation of differential solvation.[49] This question might be further considered within the framework of the ($^{-}CH_2NC$, CH_2CN^-) pair.

V. Thermochemistry

The electron affinity properly corresponds to the $|CH_2NC(v' = 0, J'K' = 0)\rangle \leftarrow |^{-}CH_2NC(v'' = 0, J''K'' = 0)\rangle$ transition. In order to obtain the adiabatic EA, we must make a rotational correction and a sequence band adjustment to the uncorrected or raw EA. These corrections have been discussed earlier[1] and will be applied here. Our final results are collected in Table V.

We make the rotational correction by treating both the ion and radical as simple prolate tops and by estimating the rotational constants (A and B) with the help of the molecular geometries in Table V. Our working expression[1] for the rotational correction is

$$\Delta_{rot} = k_B T_{rot}[(B'/B'') + (A'/2A'') - (3/2)] \qquad (6)$$

The Boltzmann constant is written as k_B and we use a rotational temperature, T_{rot}, of 500 K. The final resulting corrections turn out to be quite small; $\Delta_{rot}(^{-}CH_2NC)$ = 0.0020 ± 0.0006 eV and $\Delta_{rot}(^{-}CD_2NC)$ = 0.0010 ± 0.0005 eV. The sequence band adjustments are on the order of 0.006 ± 0.003 eV for the d_0 ion and 0.007 ± 0.003 eV for the d_2 ion. Thus we finally arrive at the corrected values for the electron affinities: EA(CH_2NC) = 1.059 ± 0.024 eV and EA(CD_2NC) = 1.070 ± 0.024 eV.

The gas-phase acidity of methyl isocyanide has been measured[11] earlier in a flowing afterglow device to be 374 ± 3 kcal/mol and has been computed[25] to be 383 kcal/mol. The gas-phase acidity is defined to be the room temperature enthalpy of the heterolytic bond dissociation.

$$H\text{-}CH_2NC \rightarrow {}^{-}CH_2NC + H^+ \qquad (7)$$

We can use the EA(CH_2NC) and the measured acidity to calculate the bond strength of methyl isocyanide.

$$DH^\circ_{298}(H\text{-}CH_2NC) = \Delta H^\circ_{acid}(H\text{-}CH_2NC) + EA(CH_2NC) - IP(H) \qquad (8)$$

We find a $DH^\circ_{298}(H\text{-}CH_2NC)$ = 84.8 ± 3.1 kcal/mol. If we employ the most recent version[50] of the heat of formation of methyl isocyanide [$\Delta H_f{}^\circ{}_{298}(CH_3NC)$ = 41.32 ± 0.24 kcal/mol], this corresponds to a heat of formation of the isocyanomethyl radical of $\Delta H_f{}^\circ{}_{298}(CH_2NC)$ = 74.0 ± 3.1 kcal/mol. Using our experimental value for the electron affinity, and assuming that the heat capacity of a free electron is 0.0, we find a value for the heat of formation of the isocyanomethide ion, $\Delta H_f{}^\circ{}_{298}(^{-}CH_2NC)$ = 49.6 ± 3.1 kcal/mol. All of these values are collected together in Table V.

An interesting comparison is to contrast the isomerizations: [HNC/HCN], [CH_3NC/CH_3CN], [CH_2NC/CH_2CN], [$^{-}CH_2NC/CH_2CN^-$], and [NH_2NC/NH_2CN]. The enthalpy of each of these rearrangement reactions except the last is now known from both experiment and the application of a uniform level of theory (Table VI). Also, the potential-energy barrier for each process has been computed and is included in the table. The only activation energy for the reactions in Table VI that has been measured[51] is 38.4 kcal/mol for CH_3NC, and this is in very good agreement with the computed value of 37.6 kcal/mol. Comparison of the measured and the computed enthalpies of reaction shows several reactions with good agreement and several where the agreement is not satisfactory; it thus seems premature to discuss

---

(46) Blackman, G. L.; Brown, R. D.; Godfrey, P. D.; Gunn, H. I. *Nature (London)* **1976**, *261*, 395.

(47) Carrick, P. G.; Engelking, P. C. *J. Chem. Phys.* **1984**, *81*, 1661.

(48) Periasamy, M. P.; Walborsky, H. M. *J. Am. Chem. Soc.* **1977**, *99*, 2631.

(49) DePuy, C. H.; Della, E W.; Filley, J.; Grabowski, J. J.; Bierbaum, V. M. *J. Am. Chem. Soc.* **1983**, *105*, 2481.

(50) Baghal-Vayjooee, M. H.; Collister, J. L.; Prichard, H. O. *Can. J. Chem.* **1977**, *55*, 2634.

(51) Collister, J. L.; Pritchard, H. O. *Can. J. Chem.* **1976**, *54*, 2380.

Table VI. Isomerization [ΔH°_{rxn}] and Activation [ΔH^*_{rxn}] Enthalpies (kcal/mol)[a]

reaction	ΔH^*_{rxn}- (calcd)	ΔH°_{rxn}- (calcd)	ΔH°_{rxn}(exptl)	ref
H—NC → H—CN	27.2	−15.3	−10.3 ± 1.1 −14.8 ± 2	52
CH_3—NC → CH_3—CN	37.6	−24.2	−23.70 ± 0.14	51
CH_2—NC → CH_2—CN	29.1	−22.0	−14.3 ± 3.7	25
$^-CH_2$—NC → CH_2=CN^-	39.7	−33.1	−25.5 ± 3.7	25
NH_2—NC → H_2N—CN	36.4	−44.9		

[a] The theoretical values are derived from "MP4/6-311++G(d,p)" calculations with scaled HF/-31+G(d) zero-point energies except CH_3CN/CH_3NC which uses scaled HF/6-31G(d) zero-point energies and HCN/HNC which is MP4-3-311++G(d,p) with scaled HF/6-31G(d) zero-point energies.

the trends in these data. There are two different values in the literature for the HNC/HCN energy difference. The first, 10.3 ± 1.1 kcal/mol, derives from an analysis[52] of the intensty of the infrared spectrum of HNC measured in a heated bath of pure HCN. The second, 14.8 ± 2 kcal/mol, derives from an ion cyclotron resonance[53] determination of the threshold for deuteron abstraction from protonated DCN. Several high-level quantum mechanical calculations of this energy difference have been performed and they uniformly favor the higher energy difference; these include values[54-56] of 14.6, 15 ± 2, and 15.0 kcal/mol. For $CH_3NC \rightarrow CH_3CN$ experimental and theoretical determinations of the energy differences agree. For CH_2NC and $^-CH_2NC$, however, the theoretical values are roughly 8 kcal/mol lower than the experimental values. This may be related to the discrepancy in the computed and measured values for the proton affinity of $^-CH_2NC$. If the measured value is too low, as these calculations suggest, then the agreement between theory and experiment for these rearrangement enthalpies would be improved.

Acknowledgment. We have had extensive conversations with Drs. A. K. Rappé, L. B. Harding, and T. H. Dunning about GVB structures for these reactive intermediates. G.B.E. thanks Argonne National Laboratory for their hospitality during a two-month visit to the Theoretical Chemistry Group at ANL. The experimental work in Boulder was supported by the United States Department of Enegy (contract No. DE-AC02-80ER10722). The VAX 11/750 digital computer used to carry out the Franck-Condon factor calculations was acquired with the help of the National Science Foundation (CHE-8407084).

---

(52) Maki, A. G.; Sams, R. L. *J. Chem. Phys.* **1981**, *75*, 4178.

(53) Pau, C.-F.; Hehre, W. J. *J. Phys. Chem.* **1982**, *86*, 321.

(54) Pearson, P. K.; Schaefer, H. F., III; Wahlgren, U. *J. Chem. Phys.* **1975**, *62*, 350.

(55) Redman, L. T.; Purvis, G. D., III; Bartlett, R. J. *J. Chem Phys.* **1980**, *72*, 986.

(56) MP4SDTQ/6-311++G(2df,2pd)//CID/6-31G(d) with scaled 6-31G(d) zero-point energies.

Cluster-Assisted Formation and Cleavage of C–H and C–C Bonds. $[Fe_3(CO)_9(CCO)]^{2-}$ and Its Acetylide and Alkyne Derivatives

Joseph A. Hriljac and Duward F. Shriver*

Contribution from the Department of Chemistry, Northwestern University, Evanston, Illinois 60208. *Received February 24, 1987*

Abstract: The ketenylidene cluster $[Fe_3(CO)_9(CCO)]^{2-}$ (**1**) is ethylated or acylated at the ketenylidene oxygen atom to generate anionic acetylide clusters $[Fe_3(CO)_9(CCOR)]^-$. The reaction of **1** with methyl trifluoromethanesulfonate generates a similar acetylide cluster and also the previously reported alkylidyne species $[Fe_3(CO)_{10}(CCH_3)]^-$. The acetylide clusters are readily protonated at low temperature to generate unstable alkyne clusters of the formula $Fe_3(CO)_9(HCCOR)$. When a solution of the ethoxyalkyne cluster is warmed to room temperature, facile cleavage of the carbon–carbon bond occurs to yield $Fe_3(CO)_9(CH)(COCH_2CH_3)$. Crystal data for $[PPN][Fe_3(CO)_9(CCOC(O)CH_3)]$: triclinic, $P\bar{1}$, $Z = 2$, $a = 10.934$ (5) Å, $b = 13.189$ (7) Å, $c = 17.075$ (6) Å, $\alpha = 84.90$ (4)°, $\beta = 70.14$ (3)°, $\gamma = 85.97$ (4)°, $V = 2305$ Å^3. Refinement of 595 variables on 4425 reflections with $I > 3\sigma(I)$ converged at $R = 4.40$ and $R_w = 4.93$.

The stabilization of reactive ligand intermediates is an important aspect of organometallic chemistry. In metal clusters there exists the added possibility that an ensemble of several metals may interact with a ligand to produce bonding modes and reactivities which are unique to the metal ensemble. The ketenylidene ligand, CCO, is an example of a ligand which is readily formed on trimetallic clusters and displays a wide range of reactivities. The behavior of the CCO moiety is greatly influenced by the identity of the metals and the charge on the cluster.

This is the first of three papers describing the chemistry of anionic ketenylidenes containing metals from the iron triad: $[Fe_3(CO)_9(CCO)]^{2-}$, $[Ru_3(CO)_9(CCO)]^{2-}$, and $[Os_3(CO)_9(CCO)]^{2-}$. These anionic clusters are highly reactive with electrophiles, but the nature of the products varies dramatically in the iron triad.

The first ketenylidene cluster was a cation, $[Co_3(CO)_9(CCO)]^+$, discovered in Seyferths' laboratory, and it was found to react with a variety of nucleophiles (eq 1).[1] In all cases the nucleophile is

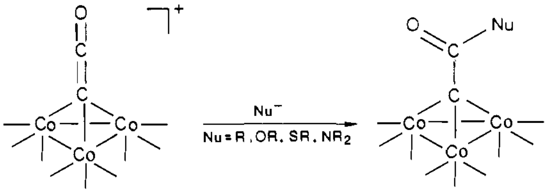

(1)

observed to attack at the β-carbon atom (the β-carbon atom is defined as the second carbon atom of the CCO ligand, i.e., $C_\alpha C_\beta O$), in reactions which are analogous to those observed for

---

(1) (a) Seyferth, D.; Williams, G. H. *J. Organomet. Chem.* **1972**, *38*, C11. (b) Seyferth, D.; Hallgren, J. E.; Eschbach, C. S. *J. Am. Chem. Soc.* **1974**, *96*, 1730.

0002-7863/87/1509-6010$01.50/0